

Investigation on vortex-induced vibration of a suspension bridge using section and full aeroelastic wind tunnel tests

Yanguo Sun^{*}, Mingshui Li and Haili Liao

*Research Centre for Wind Engineering, Southwest Jiaotong University,
Chengdu, Sichuan 610031, China*

(Received September 21, 2012, Revised April 9, 2013, Accepted May 11, 2013)

Abstract. Obvious vortex induced vibration (VIV) was observed during section model wind tunnel tests for a single main cable suspension bridge. An optimized section configuration was found for mitigating excessive amplitude of vibration which is much larger than the one prescribed by Chinese code. In order to verify the maximum amplitude of VIV for optimized girder, a full bridge aeroelastic model wind tunnel test was carried out. The differences between section and full aeroelastic model testing results were discussed. The maximum amplitude derived from section model tests was first interpreted into prototype with a linear VIV approach by considering partial or imperfect correlation of vortex-induced aerodynamic force along span based on Scanlan's semi-empirical linear model. A good consistency between section model and full bridge model was found only by considering the correlation of vortex-induced force along span.

Keywords: vortex-induced vibration (VIV); partial correlation; countermeasure; wind tunnel tests; section model; long span bridge

1. Introduction

By aerodynamics standard the main girder of long-span bridge is bluff body, periodic flow separation and wake vortices may cause it to vibrate. When the shedding frequency of vortex is close to structural natural frequency, vortex-induced vibration (VIV) may occur. Flexible line-like structures, such as tall buildings, slender chimney stacks and long-span bridges, are always suffered such kind of vibration due to its flexible, light and low damping characteristics. Larger amplitude vibrations may occur in a wind speed range called "lock-in". Various mathematical models that reflect the main mechanism of the vortex-induced response of circular cylinder have been proposed (Hartlen and Currie 1970, Iwan and Blevins 1974). A comprehensive discussion of this aeroelastic phenomenon was provided by Simiu and Scanlan (1986). In order to explore the mechanism of oscillation, Williamson and Roshko (1988) investigated the vortex shedding discipline of cylinder in detail by wind tunnel experiments. Particle imaging velocimetry (PIV) technique was used to study vortex-induced force which acted on the cylinder by Gu (1994), Rockwell (1996) and Noca (1998). Vortex shedding was reproduced and investigated, and a numerical model was developed to estimate the response of VIV on the basis of Messina Strait

^{*}Corresponding author, Ph.D., E-mail: syg222@163.com

bridge by Diana (2006). At present, it's very difficult to solve the problem of VIV of the bluff body structures theoretically as there are complex boundary conditions while solving Navier-Stokes equations. But with the advent of semi-empirical mathematic model, the problem of VIV could be described more accurately. Several two-dimensional (2-D) semi-empirical mathematic models of vortex-induced aerodynamic forces were developed after Van der Pol's oscillator model, such as models proposed by Simiu and Scanlan (1986) and Larsen (1995).

The wind-induced phenomena, particularly vortex-induced oscillations were found harmless to the safety of the structure in some occasions, but it is unacceptable considering possibly physiological impact on users of the bridge. Sometimes, it is still critical for safety if persistent vibration lasts for a long time. VIV of long span bridge is of practical interest to engineers. Therefore, a countermeasure for mitigating vibration is required. At present, wind tunnel testing for elastically mounted rigid section model becomes a general methodology to evaluate or investigate VIV performance of line-like structures, and computational fluid dynamics (CFD) method is also adopted by some researchers. Since selection of a bridge girder configuration depends on many factors such as structural and economical advantages, the basic girder shape does not necessarily have optimal aerodynamic efficiency. At present, although girder may be designed as streamlined configuration which has a good aerodynamic performance, the existence of accessories, such as rails, checking vehicle track and pavement, makes the girder prone to suffer VIV. Some long span bridges were subjected to VIV, and the corresponding countermeasures for mitigating vibration were found. Fairings, double flaps and skirt were selected as countermeasure in Trans-Tokyo Bay Bridge (Fujino 2003), and guide vanes were designed for Storebælt Suspension Bridge (Larsen 2000). The vortex response of a twin box bridge section with and without guide vanes were investigated at different Reynolds numbers (Larsen 2008). Aerodynamic countermeasures on box girder bridge section were investigated by numerical simulation method to suppress vibration (Sarwar 2010). However, such countermeasures are usually made on a case-by-case basis, which means that an effective mitigation measure for a bridge may be of deficiency to the other. It should be determined by wind tunnel tests or numerical simulation technology if possible. The best countermeasure for VIV mitigation is to find the location of girder resulted in vibration, and then to amend it instead of adding ancillary facilities (such as guide vanes, fairings, etc.).

In wind tunnel testing, 2-D or section physical model testing technique is generally adopted for investigating VIV of long-span bridge. However, the existing semi-empirical mathematic models based on wind tunnel tests or actual prototypes are all 2-D theories, and a section model in wind tunnel tests is assumed to behave in a 2-D manner, but for an actual structure, it is in reality a three-dimensional (3-D) problem. In addition to the differences in vibration mode, the aerodynamic forces are not perfectly correlated along its span. The consistence between the observation of prototype and predictions based on 2-D model testing is still uncertain due to contribution of spatial correlation of vortex-induced aerodynamic forces. Obvious oblique vortices were found in the towing tank and wind tunnel experiments by flow visualization technique (Williamson 1988, 1989, Miller 1994). Partial correlation of vortex-induced forces may be attributed partly to asynchronous trail vortices along span behind a bluff cylinder immersed in 2-D smooth oncoming flow. With considering the effect of vibration mode but ignoring the partial correlation of vortex-induced aerodynamic forces along the span, Irwin (1998), Zhu (2005), Huera Huarte (2006) and Zhang (2011) proposed some methods to estimate VIV response of the bridge. The correlation of vortex-induced force acting on square cylinders along the span was studied in detail by Wilkinson (1981), and then correlation of vortex-induced force varied with amplitude

was found through direct pressure measurement on rigid cylinder section model, and after that a double exponential correlation semi-empirical formula was fitted. On the basis of Scanlan's semi-empirical nonlinear model and Wilkinson's correlation function, Eshan (1990) discussed the vortex-induced force along the span roughly, and proposed a relatively simple method to estimate the response of VIV. Xian (2008) designed a taut stripe model of box girder to test spanwise vortex-induced response, and got the response correlation effect function to analyze the VIV of long-span bridges. A liner method which was used to estimate prototype bridge by the result of section model wind tunnel tests, was proposed by Li and Sun (2011) based on Scanlan's semi-empirical liner model.

A long-span suspension bridge with signal main cable is regarded as an engineering example in this paper. Section model and full bridge aeroelastic model wind tunnel tests for this bridge are reported in the following. Obvious VIV was observed during section model wind tunnel tests, and an optimized section configuration was found for mitigating excessive amplitude of vibration which is much larger than the one prescribed by Chinese code. In order to verify the maximum amplitude of VIV for optimized girder, a full bridge aeroelastic model wind tunnel tests with bigger scale was carried out. Great difference in vibration amplitude was found between results of section and full bridge aeroelastic model wind tunnel tests. The differences between section and full bridge model testing results are discussed based on Scanlan's semi-empirical linear model. The correlation of vortex-induced aerodynamic forces along span is studied in frequency domain at the first time, and reduced factor of vortex induced response between 2-D model to 3-D prototype structure is defined, meanwhile the methodology for extending the wind tunnel test results of section model into prototype structure by considering partial correlation of vortex-induced aerodynamic force along span is discussed. The application case of this method is provided in this paper.



Fig. 1 Effect picture of the bridge

2. Engineering background

The concerned long-span suspension bridge called Shungyong Bridge, with signal main suspended cable and steel box girder is located at Liuzhou, Guangxi province, southwest of China.

The main span of this bridge is 430 m long (layout: 40 m+430 m+40 m). The girder is 38.0 m in width, 3.5 m in depth, and with a three-lane motorway at each side. The steel tower has a unique “A” shape, and the height of the tower is 106.0 m. The special character of signal main suspended cable makes the bridge different with other typical suspension bridges, and the wind resistant performance of the bridge should be investigated in details. Figs. 1 and 2 give the details of the bridge.

It's 24.7 m height from the deck of mid-span to the lowest navigable water level. A recurrence period of 100 years was chosen by the designer in wind resistant design of the bridge. The yearly maximum mean winds averaged within 10 minutes and varied with heights and obey exponential rate. The exponent α will change with local terrain roughness. $\alpha=0.16$ is corresponding to the bridge site prescribed by Chinese Code (MOT 2004). The design wind speed is 27.7 m/s and turbulent intensity is 16% at deck level according to local meteorological data provided by Commanding Department of Shuangyong Bridge.

In order to make sure the safety of wind resistant and comfortableness of the bridge during erection and operation stage, a series of wind tunnel tests including flutter instability, aerodynamic derivatives, VIV, aerostatic instability and buffeting were conducted to assess wind-resistant performance of the suspension bridge by wind tunnel tests of section model and full aeroelastic bridge model at Research Center for Wind Engineering of Southwest Jiaotong University, Chengdu, southwest of China. This paper mainly presents the results of wind tunnel tests of VIV and discusses the consistence of section model and full bridge aeroelastic model by considering the partial correlation of vortex-induced force along span.

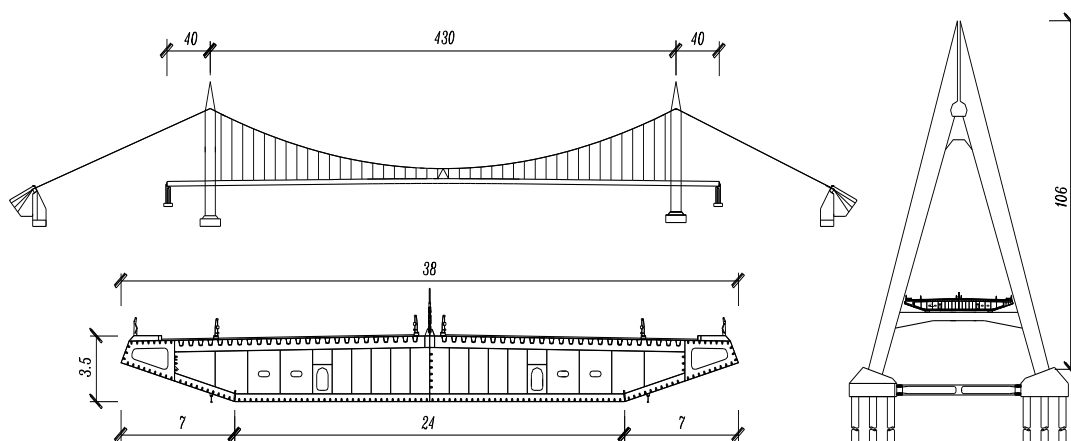


Fig. 2 General view of the single suspender bridge (Unit: m)

3. Section model testing

The objective of the section model wind tunnel testing is to verify VIV performance of the designed girder, and seek an optimized girder configuration with minimum VIV response if the amplitude of vibration is much larger than the one prescribed by Chinese code.

3.1 Model and test facility

A geometric scale 1:50 was chosen to design and manufacture the section model. The length of the model (L) is 2.095 m, the width (B) is 0.760 m and the depth (H) is 0.070 m. The ratio of length to width (L/D) is 2.757. The section model, which was designed and manufactured by using the conventional stiff model technology, was made of high quality lightweight wood and plastics. In addition to keep the similarity of geometric shape of the bridge girder, the section modeling is required to assure the similarity of mass, stiffness, and damping of structure, etc. These physical properties can be usually summarized into four dimensionless quantities: Reynolds number, Froude number, Cauchy number and critical damping ratio. Similar to the most wind tunnel tests, it is impracticable for this assignment to satisfy Reynolds number similitude. As vortex-induced resonance may occur at very low wind speed for this model scale, stiff similitude is usually replaced by Strouhal Number in the modeling to increase the onset wind speed of VIV, which should be compatible with the stable operating wind speed of wind tunnel. The other three parameters have to be employed for section modeling. Those parameters can be expressed as:

$$\begin{array}{lll} \text{Elastic parameter} & \frac{U}{f_h B} & \frac{U}{f_\alpha B} \quad U \\ \text{Mass parameter} & \frac{m}{\rho B^2} & \frac{I_m}{\rho B^4} \\ \text{Structural damping} & \zeta_h & \zeta_\alpha \end{array}$$

where, U is the wind speed; B is the width of bridge deck; f_h and f_α are vertical frequency and torsional frequency respectively; m and I_m are mass and mass moment of inertia per unit length respectively; ζ_h and ζ_α are damping ratios of structures.

The wind tunnel (Type: XNJD-1) of Southwest Jiaotong University, a closed circuit wind tunnel with two tandem closed test sections, was used to carry out the investigation. The dimension of the test section is 2.4 m×2.0 m×16.0 m ($W \times H \times L$), with wind speed adjustable from 1m/s to 45.0 m/s (turbulent intensity<0.5%). A test set-up, which was specially designed to carry out wind-induced vibration testing of bridge girder section and mounted on the outside walls of wind tunnel, was used in this investigation. The model was suspended by four pairs of linear springs and it could vibrate vertically and torsionally.

As it is known, VIV is excited by periodical vortex shedding from the sides and the tail of a bluff body when the flow passes it. Usually, the amplitude of vibration is limited and often occurs at relatively low wind speed. In order to decrease the velocity scales and increase the onset wind speed, soft springs were used in the testing. The elastically mounted model in XNJD-1 wind tunnel is shown in Fig. 3. The main parameters of the model are given in Table 1.

The first symmetrical vertical (V-S-1) and torsional (T-S-1) modes were chosen in the testing for simulating equivalent mass and mass moment of inertia. A wind speed scale of model to prototype 1:6.0 was pre-set for vertical mode, and 1:6.3 for torsional mode. As the amplitude of VIV depends strongly on structural damping, two damping levels, 0.40% (DL1) and 0.52% (DL2) were adopted to investigate possible effect of damping ratio on VIV. In order to determine the vortex-induced vibration range easily, the former damping level was set up, and the latter damping level is required by Chinese code for steel bridge. The testing was conducted in smooth oncoming

flow under three attach angles (-3° , 0° and $+3^\circ$). Two laser displacement sensors were used for acquiring the vertical and torsional amplitudes of model.



Fig. 3 View of section model in XNJD-1 wind tunnel

Table 1 The dynamic characteristics of the full scale bridge and the testing model

| Mode | Full Scale Bridge | | Testing Model | | |
|-------|-------------------|------------------------------|---------------|---------------------------|----------------|
| | Freq. | m/I_m | Freq. | m/I_m | Velocity Scale |
| V-S-1 | 0.2727Hz | 26960 kg/m | 2.34 Hz | 10.79kg/m | 6.0 |
| T-S-1 | 0.5615 Hz | 5065000 kg.m ² /m | 4.49 Hz | 0.81 kg.m ² /m | 6.3 |

3.2 Allowed amplitudes

Generally, the amplitude of VIV is limited at relatively small level, it is found to be harmless to the safety of the bridge, but the user's comfort is demanded. The comfort degree is classified to several grades depending on the acceleration of VIV in European design manual for bridges, and the amplitude of VIV in Chinese standard (MOT 2004). There are some differences existing between these two standards in low and high order vibration modes. The Chinese code is applied in this paper to evaluate the VIV performance of the suspension bridge.

In terms of Chinese code, the allowed amplitudes of the concerned bridge during service stage by referring the first vertical and torsional modes are given in following

$$\text{Vertical } [h_a] = 0.04 / f_h = 147\text{mm}$$

$$\text{Torsional } [\theta_a] = 4.56 / f_a B = 0.214^\circ$$

where $[h_a]$ and $[\theta_a]$ are allowed amplitudes of VIV according Chinese code, f_h and f_a are natural frequencies of vertical and torsional modes, B is the width of bridge main girder.

3.3 The original girder

Obvious vortex-induced oscillation or resonance was observed during testing for the model of the original girder under attack angles 0° and $+3^\circ$, and no explicit VIV was observed at attack angle -3° . Fig. 4 shows the main test results.

It is obvious that the maximum amplitudes of both vertical and torsional are much larger than the allowed ones at $+3^\circ$ attack angle. Consequently, aerodynamic optimization to cross section of girder is required to mitigate the excessive or suppress VIV response to ensure the safety and serviceability of bridge structure.

It is obvious that the maximum amplitudes of both vertical and torsional are much larger than the allowed ones at $+3^\circ$ attack angle. Consequently, aerodynamic optimization to cross section of girder is required to mitigate the excessive or suppress VIV response to ensure the safety and serviceability of bridge structure.

3.4 Aerodynamic optimization of the girder

In order to suppress the excessive amplitude of VIV of the bridge, reasonable and convenient aerodynamic optimization for girder section is required. As it is necessary to keep the main configuration of box girder unchanged even in preliminary design stage, a series of tests were then arranged for altering geometric parameters of accessories of girder including the position of checking vehicle tracks, gaps between the track and bottom of girder, the position of pavement and its height and porosity of railing and so on. All tests were first conducted under lower damping level (DL1) and $+3^\circ$ attack angle. A comprehensive description of all aerodynamic optimizations for the girder is summarized in Table 2.

An optimized section configuration was found during a series of wind tunnel tests (the 8th measure in Table 3). The changes in the optimum countermeasure include decreasing the height of pavement to 25cm, setting the dip angle at 45° , installing checking vehicle tracks 144cm from the joint of bottom plate, and setting the gaps between track and the bottom plate to 10cm. In addition, the porosity of railing is increased by 10%. The optimized section configuration details are shown in Fig. 5.

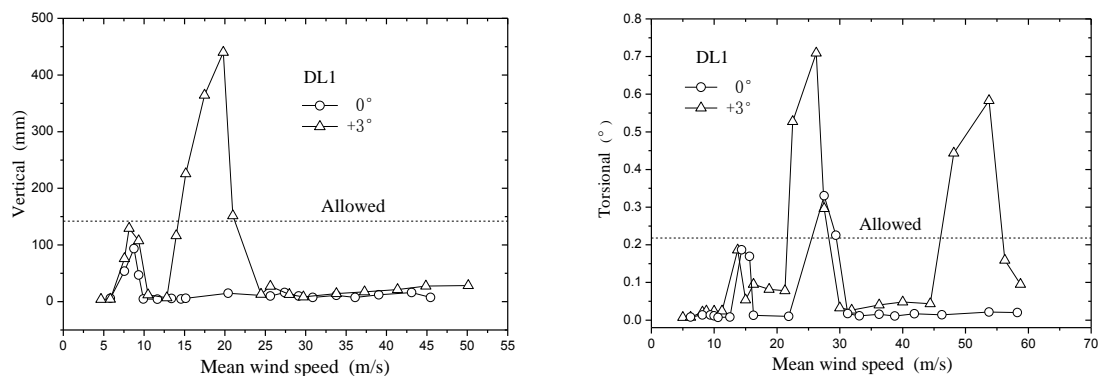
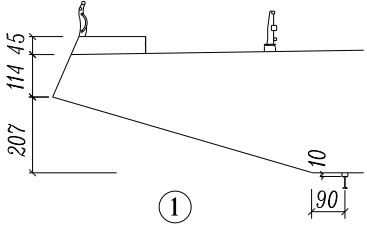
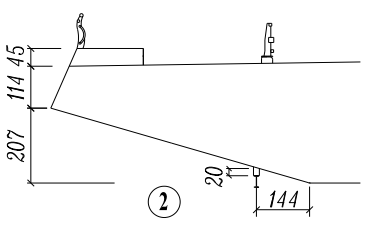
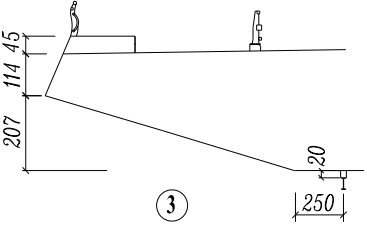
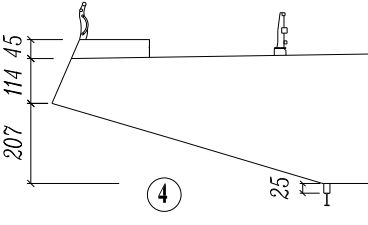
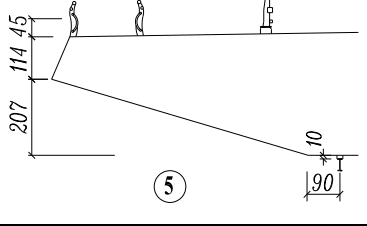
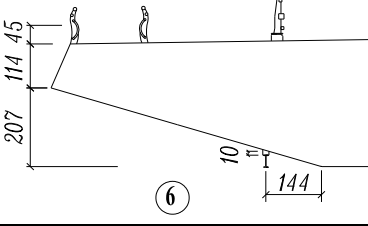
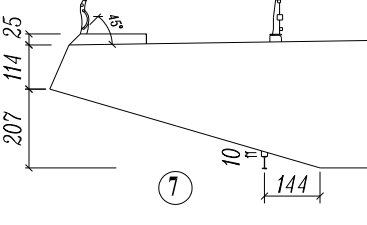
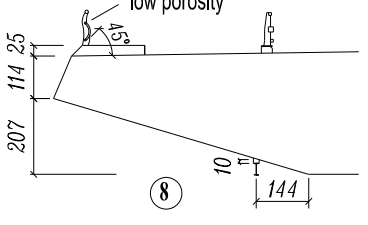


Fig. 4 Full scale VIV amplitude versus wind speed

Table 2 VIV amplitudes of aerodynamic measures

| Aerodynamic measure | Amplitude (mm/°) | Aerodynamic measures | Amplitude (mm/°) |
|---|----------------------------|--|----------------------------|
|  | V 122.7 421.4 T 0.68 |  | V 145.4 406.2 T 0.99 |
|  | V 121.9 414.9 T 0.91 |  | V 134.3 440.3 T 0.90 |
|  | V 202.9 504.8 T 0.71 |  | V 138.9 343.1 T 0.32 |
|  | V 150.5 345.1 T 0.73 |  | V 131.8 212.0 T 0.03 |

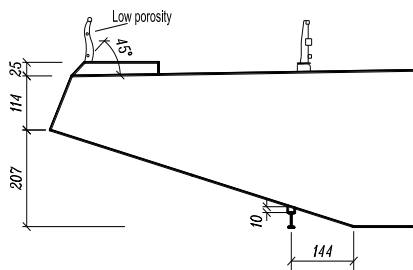


Fig. 5 The optimized section configuration (Unit: cm)

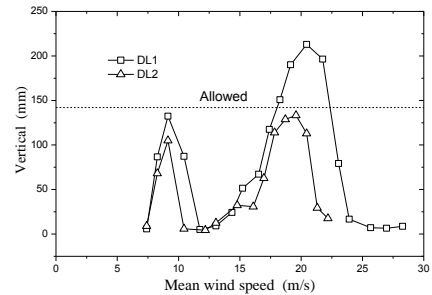


Fig. 6 Full scale VIV amplitude (attack angle: +3°)

Tests were also conducted at higher damping level (DL2) to verify its performance. Test results of this measure at two different damping levels are shown in Fig. 6. It is noted that no explicit torsional VIV was observed during tests, and obvious vertical VIV was still observed, but the maximum vertical VIV amplitude was reduced and meets the requirement of Chinese code at higher damping level (DL2). No obvious vibration was found at 0° and -3° , thus the implicit amplitudes were not shown in the paper.

4. Full aeroelastic bridge model testing

The integrated effect of girder, tower and cable can be fully considered by full bridge aeroelastic model, which reflects the interaction between bridge and wind more correctly. It's the best approach to investigate VIV performance of long-span suspension bridge. But the VIV phenomenon has been observed scarcely in the past full bridge wind tunnel tests, which is common in section model tests, because of the small scale (about 1:100) or other factors beyond control. Therefore, in order to verify the results of VIV for optimized girder proposed by section model testing, the larger scale of full bridge model is needed. The bigger dimensions of the model make the details of the girder and other parts of the bridge (i.e. railing, checking vehicle track, wind fairing etc.) more precise and clear, and testing results more credible.

The VIV performances of the bridge in smooth and turbulent flow were all investigated, and the test results in smooth flow are mainly presents in this paper.

4.1 Model and test facility

The testing for full bridge aeroelastic model was carried out in XNJD-3 wind tunnel of Southwest Jiaotong University. It is a closed circuit type wind tunnel, and the test section dimension is $22.5 \text{ m} \times 4.5 \text{ m} \times 36 \text{ m}$ ($W \times H \times L$), and the wind speed can be adjustable between 0.5-16.5 m/s. The turbulent intensity of oncoming flow is less than 1.0% in empty case (Li 2009). A larger geometrical scale 1:60 was chosen to simulate the required details of the long span bridge and just yielded blockage less than 2.0% which meets the testing conditions (Generally, the blockage should be less than 5% for the wind tunnel testing). The layout of model in wind tunnel is show in Fig. 7. This test section is equipped with atmospheric boundary layer simulation setup, which is composed of spires, fence and cubes etc. The setup covers roughly 25 m long at floor of the wind tunnel (Usually, the coverage length of boundary layer setup is six times of spire height to ensure a rational turbulent field). This setup can generate the wind exposures (wind profiles, turbulent profiles, wind spectra and length scales) required by Chinese code or other design standard. The quality of the uniform flow field is concerned in this paper as VIV typically occurs in the low turbulence intensity flow.

According to the similarity theory, except for Reynolds number which is unable to satisfy similitude, the other four parameters have to be satisfied for the full bridge aeroelastic modeling. Those parameters are clarified as following:

$$\text{Elastic parameter} \quad \frac{EA}{\rho U^2 B^2}, \quad \frac{EI}{\rho U^2 B^4}, \quad \frac{EK}{\rho U^2 B^4}$$

Mass parameter $\frac{m}{\rho B^2}, \frac{I_m}{\rho B^4}$

Damping parameter ζ

Gravity parameter $\frac{gB}{U^2}$

in which, ρ is air density; U is the mean wind speed; B is the width of bridge deck; g is the gravity acceleration; μ is the air viscous coefficient; EA , EI and GK are the extension stiffness, bending stiffness and free torsion stiffness; m and I_m are mass and mass moment of inertia per unit length.

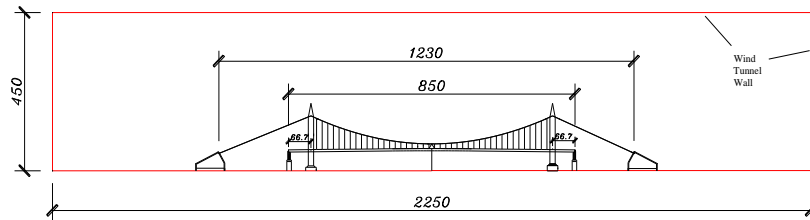


Fig. 7 Model layout in wind tunnel (XNJD-3 Unit: cm)

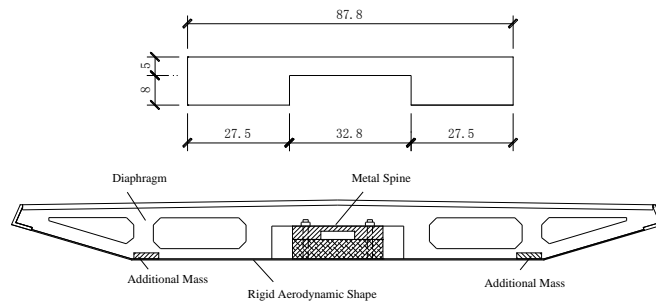


Fig. 8 Metal spine of main girder (Unit: mm)

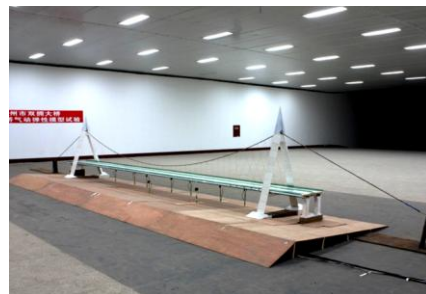
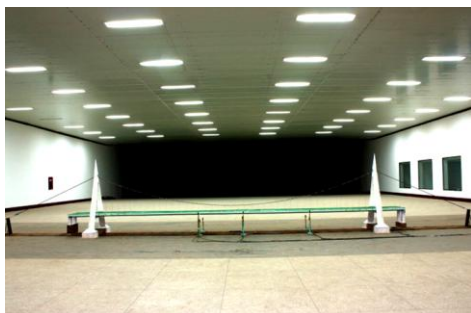


Fig. 9 View of full bridge model at XNJD-3 wind tunnel

In terms of the similitude parameters above, the scales of wind speed, acceleration and frequency are $C_u = 1/\sqrt{60} = 1:7.75$, $C_a = 1:1$ and $C_f = \sqrt{60}/1 = 7.75:1$ respectively. However, it is noted that the damping ratio is not known exactly until the structure comes into existence. It is necessary to make sure the damping ratio of model is lower than 0.5% which is prescribed by Chinese code.

The aeroelastic model of the completed bridge is composed of the girder, towers, stayed cables, pavement and railing etc. The aeroelastic model of the bridge during erection does not have railing. The full bridge model was designed and manufactured by using the conventional aeroelastic model method. The structural stiffness of main girder and the towers was provided by a metal spine assembly; the external shape was provided by cladding elements and mass was provided by lumping complimentary ballast elements in the cladding structure (see Fig. 8). Channel steel was adopted for metal spine of main girder, and rectangular steel for tower. To avoid the extra stiffness provided by the cladding element, the main girder was divided into 26 sections. There was 2 mm gap between two sections. The similar dividing method was adopted for tower. The main cable was simulated by steel wire strand and lead bricks. For the railing, only their geometric shapes were simulated. The total length of the girder model is 8.5 m, and the height of the tower is 1.78 m. Fig. 9 shows the details of full bridge model in wind tunnel. This manufacture method makes it possible to measure external structural displacements by using displacement or acceleration transducers and sectional forces by strain gauges attached to the spine structure.

A hot-wire anemometry was used to measure the simulated wind field. The wind induced displacement was measured by using laser displacement sensors at each 1/8 span.

4.2 Flow field measurement

It is a routine to conduct a testing to calibrate the flow field of bare wind tunnel. The flow field measurement was conducted at nominal wind speed 10.4m/s and the data was acquired for each measurement location at sampling frequency of 256 Hz for 40s. The wind speed was measured with a single-wire, hot-wire anemometer (DANTEC) at height level 1.05 m and 0.45 m.

The mean wind speed data of empty tunnel at eight different testing sites is shown in Fig. 10. It is noted that the variation of mean wind speed is less than 1.5% relative to the average mean wind speed, and meets the testing requirement well.

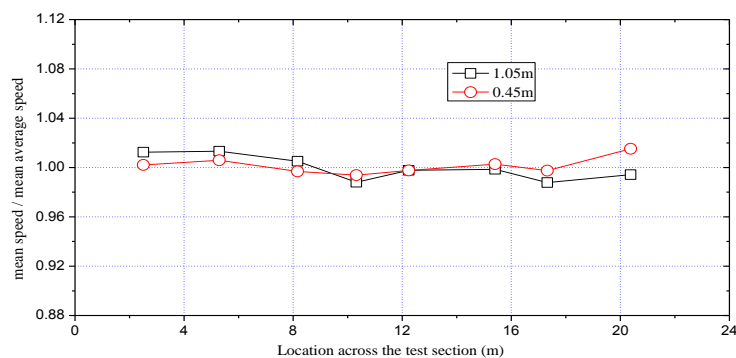


Fig. 10 Variation of mean wind speed across test section for bare wind tunnel

4.3 Simulation for nonzero attack angle

The testing was conducted in smooth and simulated boundary layer oncoming flow under two yaw angles 0° , 15° and two attack angles 0° , $+3^\circ$ respectively. Usually, full bridge aeroelastic model wind tunnel tests can only simulate 0° wind attack angle, while the simulation of other kind of wind attack angle has too much difficulties. There are some immature simulation methods to be chosen when the wind-induced vibration of structure under other attack angles need to be paid attention to, such as the attack angle panel simulation method and the overall model booster method. The attack angle panel simulation method needs to design a certain height trapezoidal plate, depending on the height of the bridge site, so that a flow field of certain angle would be generated when the wind passes through the plate. The overall model booster method makes the use of some certain wedge-shaped wood to booster the overall model under each bearing, then a certain attack angle acting on the test model would be created to achieve the attack angle simulation. However, both simulation methods have some unavoidable flaws. The overall model booster method is simple, but this method will change the structure, and the damping ratio is hard to determine when aeroelastic model is transformed into the other angle of attack, which is only regarded as a mean of qualitative analysis method. The attack angle panel method have to design different attack angle simulation equipment under different conditions depending on the height of the bridge site, and other disadvantages such as time-consumption, cost, and change for the flow field of turbulent flow should also be taken into consideration. But the smooth flow is slightly affected by this method.

In this paper, the attack angles $+3^\circ$ was simulated by the attack angle panel method (see Fig. 8). The shape and dimensions of the equipment were designed by CFD numerical simulation technology, and then verified by flow calibration testing (see Fig. 11). The flow field of this wind tunnel was simulated by CFD at different wind speed. Analysis showed that the attack angles of flow varied slightly with oncoming wind speed. Fig. 12 shows the angles of flow around the panel. The main girder of full bridge model was arranged within the area about 3° attack angle, to achieve the simulation of wind attack angle.

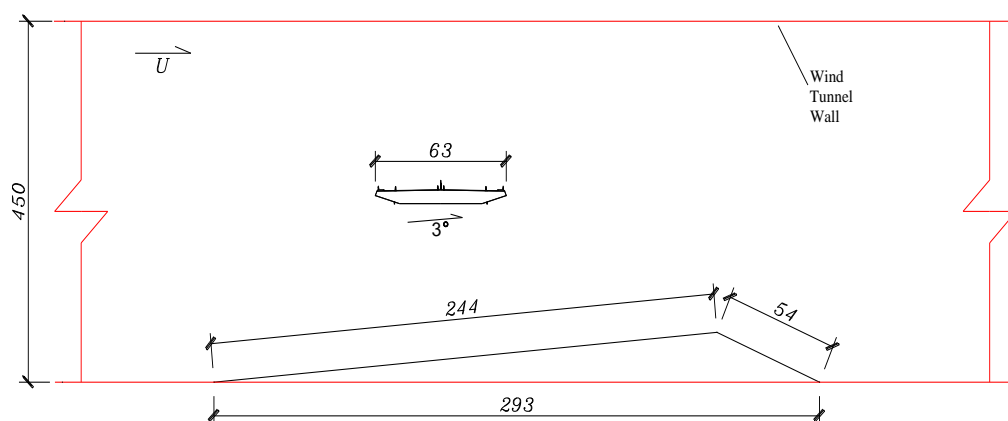


Fig. 11 Equipment for changing attack angle (Unit: cm)

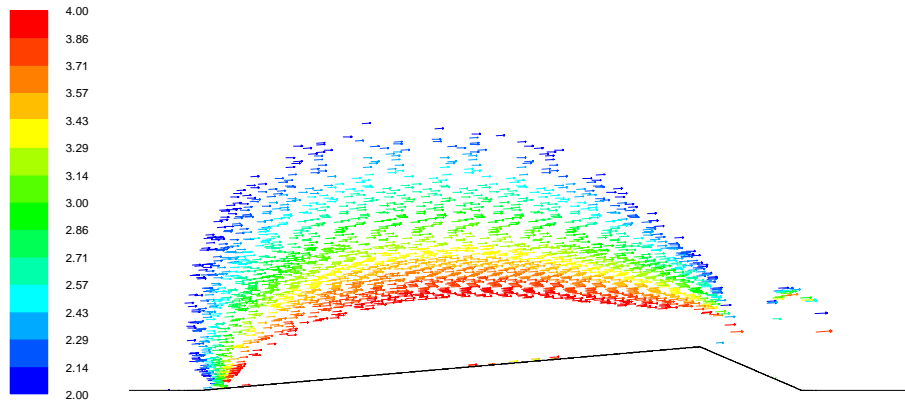


Fig. 12 Wind attack angles at 4 m/s

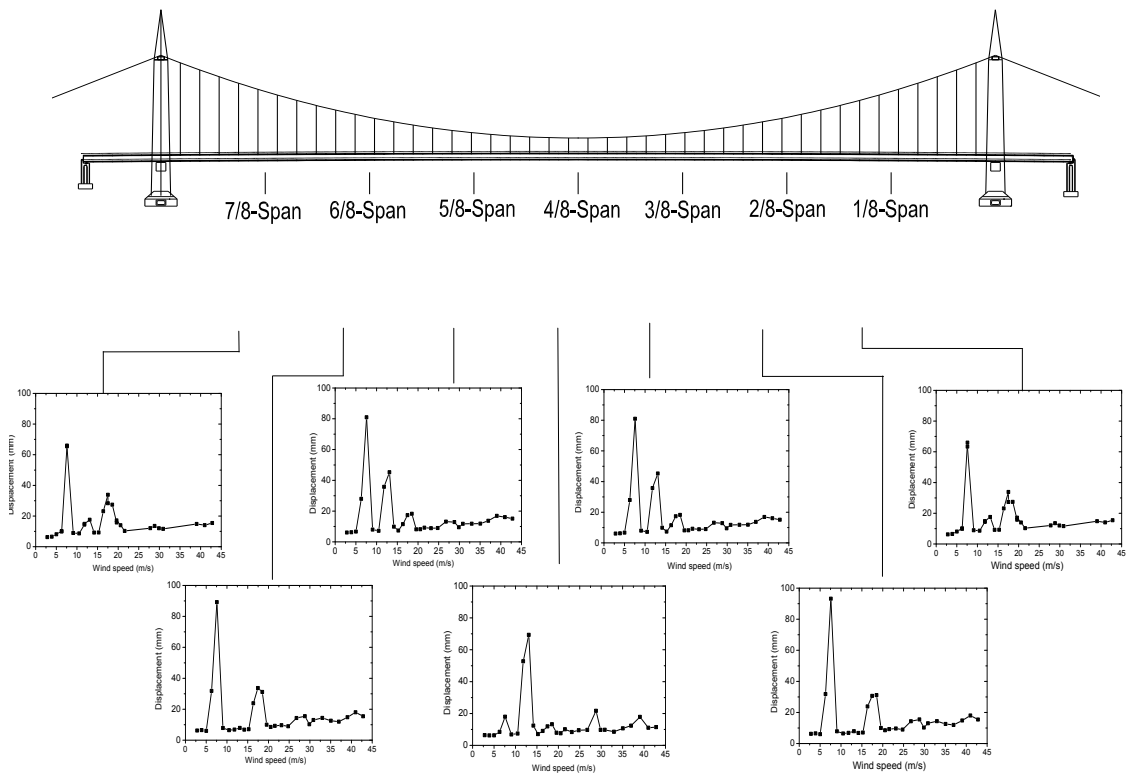


Fig. 13 VIV amplitude varies with wind speeds at seven measured locations

4.4 Verification of dynamic properties

It is necessary to verify the simulated dynamic properties of the full bridge model under “no wind” environment before commencement of the tests. The dynamic properties (mode shapes, frequencies, structural damping) of the full aeroelastic bridge model were measured with the forced vibration method. Acceleration transducers were used to acquire the vibration signals in the tests.

For a given mode, its frequency and structural damping can be found by calculating the mechanical admittance between response (acceleration) and the forced vibration signal as the input. At least two acceleration transducers were used for identification of mode shape. The relative amplitudes and phases were measured through the admittance function between two transducers by keeping one transducer stationary at mid-span or 1/4 span and successively moving the other transducer horizontally at an interval of one section of the main girder thereon to a spacing of the end of back span. Table 3 gives the main concerned dynamic characteristics of the full bridge model. The frequencies of principal modes are close to the required ones, and the damping ratio is within a reasonable range.

4.5 Test results

Explicit VIV responses were observed only for the bridge under smooth oncoming flow at +3° attack angle. Table 4 summarizes the results of maximum amplitudes and wind speeds while oscillation occurred, and Fig. 13 shows VIV amplitude varies with wind speeds at seven measured locations. As the design wind speed at deck level is 27.73 m/s, the torsional VIV can be ignored due to its high “lock-in” wind speed. It is also found that testing results at yaw angle 0° were different with 15° according to the following table. This indicates that skew wind has slight effect on “lock-in” wind speed, especially, the maximum VIV amplitude increases slightly, which could not be observed in section model testing. However, the maximum amplitude still meets the requirement of Chinese code.

No obvious VIV was observed during the model testing under simulated boundary layer flow (turbulence intensity is 16%). The test results are reasonable due to the presence of higher turbulent intensity in oncoming flow, which brings positive result.

Table 3 Dynamic characteristics

| Mode shape | Prototype freq. (Hz) | Model freq. (Hz) | Damping ratio (%) |
|------------|----------------------|------------------|-------------------|
| V-S-1 | 0.281 | 2.244 | 0.37 |
| V-A-1 | 0.299 | 2.358 | 0.35 |
| T-S-1 | 0.55 | 4.341 | 0.43 |
| V-S-2 | 0.554 | 4.425 | 0.46 |
| T-S-2 | 0.626 | 5.661 | -- |
| V-A-2 | 0.855 | 7.421 | -- |

Note: V-vertical, T-torsional, S-symmetric, A-asymmetric. E.g. V-S-1 represents the first symmetrically vertical bending mode.

Table 4 The maximum amplitude of VIV at +3° attack angle

| Item | Yaw angle (°) | Mode | Wind speed (m/s) | Maximum VIV amplitude | | |
|------------------|--------------------|-------|-----------------------|-----------------------|----------|----------|
| | | | | 1/2-span | 3/8-span | 1/4-span |
| Vertical (mm) | 0 | V-A-1 | 7.58 | 17.81 | 80.16 | 92.26 |
| | | V-A-2 | 18.53 | 9.28 | 12.77 | 31.16 |
| | | V-S-1 | 13.1 | 68.94 | 44.78 | 7.85 |
| | | V-S-2 | 28.80 | 15.16 | 9.01 | 10.86 |
| | 15 | V-A-1 | 9.05 | 27.18 | 103.43 | 122.67 |
| | | V-A-2 | 18.53 | 6.52 | 9.2 | 21.22 |
| | | V-S-1 | 14.17 | 77.33 | 50.28 | 6.75 |
| | | V-S-2 | 24.77 | 31.79 | 23.56 | 12.99 |
| Torsion (°) | 0 | T-S-1 | 32.10 | 0.332 | 0.307 | 0.229 |
| | 15 | T-S-1 | 32.10 | 0.450 | 0.441 | 0.321 |
| | | T-S-2 | 65.750 | 0.168 | 0.165 | 0.130 |

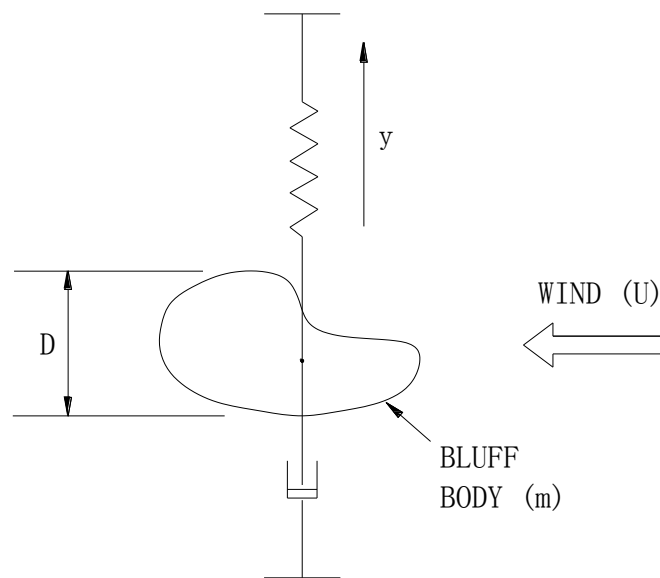


Fig. 14 Mathematical model for elastically mounted bluff body

5. Discussion on consistency of model tests

Great differences exist between section model and full bridge aeroelastic model testing results. The correlation of vortex-induced force along the span may account for this difference. There is still lack of comprehensive approach to extend the test results of section model into prototype bridge because of the fact that the existence of mode shapes and the nonlinear vortex-induced forces are not fully correlated along the span, although several researchers tried to study it (Ehsan 1990, Zhu 2005, Huera Huarte 2006, Xian 2008).

A linear VIV approach by considering partial or imperfect correlation of vortex-induced aerodynamic force along span on the basis of Scanlan's semi-empirical linear model is proposed in the following. The correlation of vortex-induced aerodynamic force along span is studied, and amplitude reduced factor of vortex induced response between 2-D to 3-D is defined in this method.

5.1 Linear model description

The sketch of mathematic model for VIV mechanism is shown in Fig. 14. By considering the existence of phase-difference along the span, the across-flow VIV of a rigid bluff body based on Scanlan's semi-empirical linear force model (Scanlan 1986) should take the following form (here take the lift for example)

$$m(\ddot{y} + 2\zeta\omega_0\dot{y} + \omega_0^2y) = \frac{1}{2}\rho U^2 D [Y_1(K)\frac{\dot{y}}{U} + Y_2(K)\frac{y}{D} + \frac{1}{2}C_L(K)\sin(\omega t + \psi(x))] \quad (1)$$

in which, m is mass of per unit span length; ζ is damping ratio-to-critical; ω_0 is mechanical circular frequency; ρ is air density; U is the velocity of wind flow; D is across-flow dimension of section; $y(x, t)$ is the vortex-induced response displacement of the bluff body, x is along-span degree-of-freedom; $K = \omega D/U$, ω is vortex shedding frequency that satisfies the Strouhal relation $2\pi S = \omega D/U$ (S is Strouhal number); parameters need to be determined are $Y_1(K)$, $Y_2(K)$, $C_L(K)$, $\psi(x)$. Simiu and Scanlan (1986) proposed a method to identify the parameters by wind tunnel tests.

Introducing generalized coordinates, the vertical motion y at the spanwise location x of the deck coordinate at any time t may be expressed as

$$y(x, t) = \phi(x)\xi(t)D \quad (2)$$

in which, $y(x, t) = \phi(x)\xi(t)D$, $\phi(x)$ is non-dimensional mode shape and $\xi(t)$ is its generalized coordinate. D is the dimension in across-flow.

Let $s = \frac{Ut}{D}$ and $K_0 = \frac{\omega_0 D}{U}$. The non-dimensional form of the mathematical model can be written as the following equation by inserting Eq. (2) into the original form Eq. (1), multiplying both sides by $\phi(x)$, and integrating over the length L of the span

$$\ddot{\xi}(s) + (2\zeta K_0 - \frac{\rho D^2}{2m_{eq}} Y_1)\dot{\xi}(s) + (K_0^2 - \frac{\rho D^2}{2m_{eq}} Y_2)\xi(s) = \frac{\Gamma F(s)}{g} \quad (3)$$

in which, $\varrho = \frac{1}{L} \int_{-L/2}^{L/2} \phi^2(x) dx$; $m_{eq} = \frac{M}{L\varrho}$; $M = \int_{-L/2}^{L/2} m(x)\phi(x)^2 dx$; $F(s) = \frac{1}{L} \int_{-L/2}^{L/2} |\phi(x)| \sin[Ks + \psi(x)] dx$
and $\Gamma = \frac{\rho D^2 C_L}{4m_{eq}}$.

$F(s)$ can be written in the form

$$F(s) = \frac{1}{L} \int_{-L/2}^{L/2} |\phi(x)| f(s, x) dx \quad (4)$$

in which, $f(s, x) = \sin[Ks + \psi(x)]$.

The correlation of $F(s)$ along the span is first studied in frequency domain here, and the correlation of $F(s)$ can be expressed as

$$R_{F(\tau)} = \frac{1}{L^2} \int_{-L/2}^{L/2} \int_{-L/2}^{L/2} |\phi(x_1)| \cdot |\phi(x_2)| R_{f(\tau)} dx_1 dx_2 \quad (5)$$

Fourier transform is applied in both sides of above equation

$$S_F(\omega) = \frac{1}{L^2} \int_{-L/2}^{L/2} \int_{-L/2}^{L/2} |\phi(x_1)| \cdot |\phi(x_2)| \cdot S_f(\omega, |x_2 - x_1|) dx_1 dx_2 \quad (6)$$

Correlation function of 3-D spectrum can be written as a general form proposed by Houblt (1958)

$$R(M, M', \omega) = \frac{S_F(M, M', \omega)}{S(\omega)} \quad (7)$$

where M and M' represent any two points of 3-D space respectively, Eq. (6) can be rewritten as follow by using above Eq. (7)

$$S_F(\omega) = \frac{1}{L^2} \int_{-L/2}^{L/2} \int_{-L/2}^{L/2} |\phi(x_1)| \cdot |\phi(x_2)| \cdot R(\omega, |x_2 - x_1|) S(\omega) dx_1 dx_2 \quad (8)$$

where $S(\omega)$ is power spectrum of vortex induced force at any certain point of span. According to the Wilkinson's expression, correlation function R is independent with frequency ω , because the mode shapes of vortex induced vibration are separated each other at lock-in. Strouhal number is constant within a specified range. (Because VIV is of single frequency vibration, the assumption of correlation function is independent with frequency is reasonable). Eq. (8) can be written as the following simplified form

$$S_F(\omega) = R_F S(\omega) \quad (9)$$

$$R_F = \frac{1}{L^2} \int_{-L/2}^{L/2} \int_{-L/2}^{L/2} |\phi(x_1)| \cdot |\phi(x_2)| R(|x_2 - x_1|) dx_1 dx_2 \quad (10)$$

Auto-convolution integral of mode shape in Eq. (8) is pre-defined as the following form (Li and Tanaka 1996)

$$\theta(\Delta x) = 2 \int_{-L/2}^{L/2-\Delta x} |\phi(x)| \cdot |\phi(x + \Delta x)| dx \quad (11)$$

Squaring root of both sides of Eq. (9), the reduced relation of vortex induced forces between 2-D and 3-D is $F = \Phi \cdot f$. After inserting Eq. (11) into (10) and extracting square root both sides of Eq. (9), and reduced factor Φ of vortex induced force between 2-D and 3-D can be defined as

$$\Phi = \frac{1}{L} \sqrt{\int_0^L \theta(\Delta x) R(\Delta x) d\Delta x} \quad (12)$$

in which, $R(\Delta x)$ is correlation function of vortex-induced aerodynamic force along span, Δx is spacing along span length L . It is obvious that reduce factor varies with length of model and amplitude and the values belong to the range of (0, 1).

The Eq. (3) can be rewritten as the following form based on above analysis

$$\ddot{\xi}(s) + (2\zeta K_0 - \frac{\rho D^2}{2m_{eq}} Y_1) \dot{\xi}(s) + (K_0^2 - \frac{\rho D^2}{2m_{eq}} Y_2) \xi(s) = \frac{\Gamma \Phi \sin[Ks + \psi_0]}{g} \quad (13)$$

The simplified form of Eq. (13) can be written as follow

$$\ddot{\xi}(s) + 2\gamma \hat{K}_0 \dot{\xi}(s) + \hat{K}_0^2 \xi(s) = \frac{\Gamma \Phi}{g} \sin[Ks + \psi_0] \quad (14)$$

where $2\gamma \hat{K}_0 = 2\zeta K_0 - \frac{\rho D^2}{2m_{eq}} Y_1$; $\hat{K}_0^2 = K_0^2 - \frac{\rho D^2}{2m_{eq}} Y_2$.

The amplitude of the generalized coordinate can be expressed like this

$$\xi(s) = \frac{\Gamma \Phi}{g \hat{K}_0^2} \frac{\sin[Ks - \theta]}{\sqrt{(1 - \beta_v^2)^2 + (2\gamma \beta_v)^2}} \quad \theta = \arctan \frac{2\gamma \beta_v}{1 - \beta_v^2} \quad (\beta_v = K / \hat{K}_0) \quad (15)$$

The VIV amplitude of the concerned structure with considering the partial correlation can be obtained by Eq. (2), that is $y = \xi_0 D$.

5.2 Application of linear method

Due to the lack of exact expression of correlation function for a certain concerned bridge girder, the correlation function proposed by Wilkinson (1981) based on direct pressure measurement on cylinder of square is used in present analysis

$$R(\Delta x) = \exp[-f_1(\eta) (\frac{\Delta x}{D})^{f_2(\eta)}] \quad (16)$$

in which, η is non-dimensional amplitude of vibration, $f_1(\eta)$ and $f_2(\eta)$ can be fitted as the following functions (Ehsan 1990)

$$f_1(\eta) = \frac{0.052}{0.298 + \eta^{0.25}}; \quad f_2(\eta) = \frac{0.065}{0.042 + \eta} \quad (17)$$

Fig. 15 shows the examples of correlation curves based on Wilkinson's research. It's obvious that correlation function of vortex-induced force varied with amplitude and spacing along span.

For section model case, the reduced factor varies with length of model and amplitude. The mode shape function is $\phi(x)=1$, $\theta(\Delta x)$ and $R(\Delta x)$ can be computed by Eqs. (11) and (16) respectively. The reduced factor Φ can be obtained from Eq. (12). Fig. 16 shows the reduced factors of section model vary with length of model and amplitude. For prototype or full bridge aeroelastic model of long span suspension bridge, the mode shape function of first symmetric vertical mode (V-S-1) can be approximately expressed as $\phi(x) = \cos(\pi \cdot x/L)$, and $\phi(x) = \sin(2\pi \cdot x/L)$ for first asymmetric vertical mode (V-A-1). The reduced factors can be obtained from above mentioned equations too. Figs. 17 and 18 show that the reduced factors for prototype bridge or full bridge aeroelastic model vary with length and amplitude at different modes.

If all required similitude including mass, stiffness and damping is followed, the amplitude derived from section model testing can be interpreted into prototype bridge by the following iteration equation

$$A_{pi+1} = nA_m \cdot \frac{\Phi_{pi} \mathcal{G}_m}{\Phi_m \mathcal{G}_p} \quad (18)$$

in which, n is model scale, A is amplitude, m and p represent model and prototype, i represents iteration time, \mathcal{G} was defined in Eq. (3).

The iteration procedure is provided as follows:

1) Get the value of A_m from section model wind tunnel tests, and then get the reduction factor of section model Φ_m through Eq. (12).

2) First, let the prototype bridge amplitude $A_{p1} = n \cdot A_m$, get the reduction factor Φ_{p1} of the bridge at certain mode by using Eq. (12).

3) Get the prototype bridge amplitude A_{p2} from Eq. (18) by using the section model parameters and Φ_{p1} , and then get reduction factor Φ_{p2} of the bridge at certain mode through Eq. (12).

4) The amending for mode shape in this method has been finished in the first iterative process, and it shouldn't be included in the rest iterative processes. It means that the iterative equation of the rest processes can be written as

$$A_{pi+1} = nA_m \frac{\Phi_{pi}}{\Phi_m} \quad (19)$$

Finally, the maximum amplitude of prototype bridge or full bridge model can be computed by Eqs. (18) and (19) after several iterative processes.

Because the damping of section model is different with the damping of prototype bridge or full bridge model, the VIV amplitude of Shuangyong bridge must be modified before it is taken as

example in this section. A modification method was proposed by Zhu (2005) which the partial correlation of vortex-induced force along the span was not taken into account, the correction coefficient of damping between the sectional model and the prototype bridge in this method is presented as

$$A_p = C_\xi A_m \quad (20)$$

in which, subscripts p and m represent prototype bridge and model; C_ξ is so called correction coefficient of damping, which can be calculated by following equation

$$C_\xi = (\xi_p (1 - \xi_p^2)^{0.5})_p / (\xi (1 - \xi^2)^{0.5})_m \quad (21)$$

in which, ξ is damping ratio.

After following Eq. (20), the VIV amplitude derived from section model testing is 3.65 mm (182.3 mm for prototype case) at damping level 0.5% which is required by Chinese code, and the vibration amplitudes derived from full bridge aeroelastic model testing directly are modified at damping level 0.5% as well, one can yield 64.5 mm for mode V-A-1, and 51.1 mm for mode V-S-1. The significant difference is observed between section model and full bridge aeroelastic model testing. By using the iteration Eq. (18) and the results of section model testing, the amplitudes of prototype bridge can be predicted after several iteration times, i.e., 52.1 mm for mode V-A-1, and 50.4 mm for mode V-S-1. The modified results are very close to the results of full bridge aeroelastic model wind tunnel tests.

It's obvious that a good consistency between section model and full bridge model is only found by considering the contribution of correlation of vortex-induced force along span. Therefore, the predicted amplitude by using section model testing result is conservative and roughly 2 times larger than the one based on full bridge model testing. The same finding was also reported by Ehsan (1990).

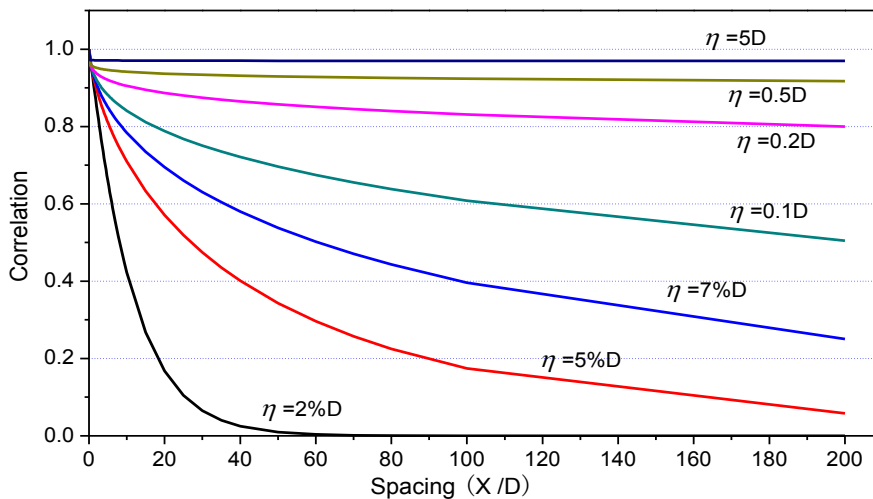


Fig. 15 Examples of correlation curves (Wilkinson, 1981); Symbol: η =amplitude; D =depth of girder

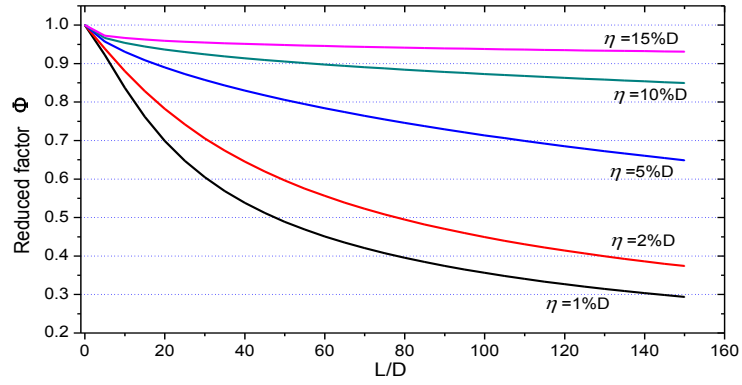


Fig. 16 Reduced factors for section model ($\phi(x) = 1$)

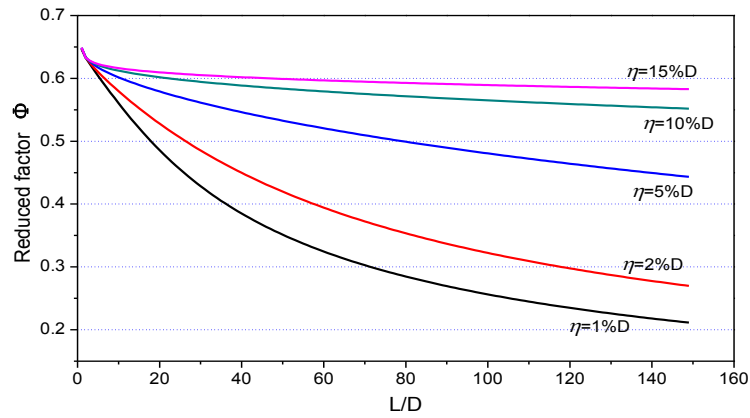


Fig. 17 Reduced factors for suspension bridge (V-S-1)

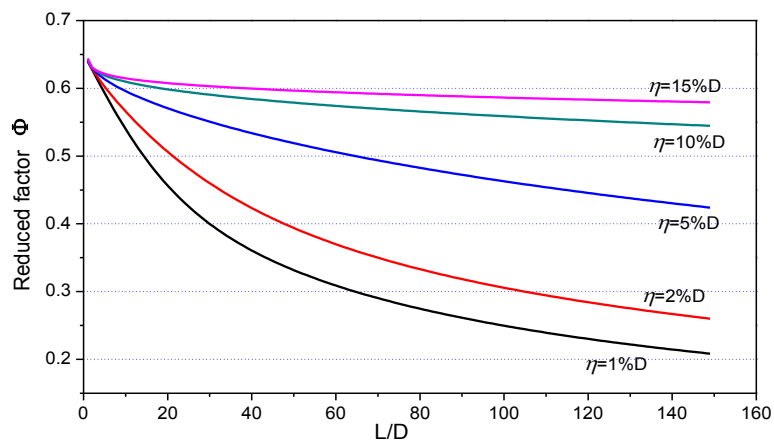


Fig. 18 Reduced factors for suspension bridge (V-A-1)

6. Conclusions

The section model wind tunnel tests were reported about VIV of a single main cable suspension bridge and its mitigation countermeasures. A large scale full bridge aeroelastic model wind tunnel test was carried out to verify the maximum amplitude of VIV for optimized girder. The difference of section and full aeroelastic model testing results was discussed by considering the correlation of vortex-excited force along the span. A relatively simple linear method for predicting VIV response of long-span bridge has been outlined based on section model testing results. The proposed linear method for estimating the vortex-induced response of long-span bridge appears to yield reasonable results without complex computation and numerical simulation. The good consistency between section model and full bridge model was only found by accounting for the contribution of correlation of vortex-induced force along span.

It is worth paying attention to that the nonlinear characters of vortex-induced force and the correlation function of realistic bridge girder were not taken into account. The proposed method can be extended to analyze torsional vortex induced vibration.

Acknowledgements

Financial support from National Natural Science Foundation of China (Project No. 50978223), National Natural Science Foundation of China (Project No. 51278435), Major State Basic Research Development Program of China (973 Program) (Project No. 2013CB036301), and Commanding Department of Shuangyong Bridge at Liuzhou, Guangxi are gratefully acknowledged.

References

- Diana, G., Resta, F., Belloli, M. and Rocchi, D. (2006), "On the vortex shedding forcing on suspension bridge deck", *J. Wind Eng. Ind. Aerod.*, **94**, 341-363.
- Ehsan, F. and Scanlan, R.H. (1990), "Vortex-induced vibrations of flexible bridges", *J. Eng. Mech - ASCE*, **116**(6), 1392-1410
- Fujino, Y. (2003), *Wind resistant design of bridges—code practice and recent developments*, Structural Engineering Series 12, JSCE.
- Gu, W., Chyu, C. and Rockwell, D. (1994), "Timing of vortex formation from an oscillating cylinder", *Phys. Fluids*, **6**, 3677-3682.
- Hartlen, R.T. and Currie, I.G. (1970), "Lift-oscillator model of vortex-induced vibration", *J. Eng. Mech. - ASCE*, **96**(5), 577-591.
- Houblt, J.G. (1958), *On the response of structural having multiple random inputs*, WGLR-Jahrbuch 1957.
- Huera Huarte, F.J., Bearman, P.W. and Chaplin, J.R. (2006), "On the force distribution along the axis of a flexible circular cylinder undergoing multi-mode vortex-induced vibrations", *J. Fluid Struct.*, **22**, 897-903.
- Irwin, P.A. (1998), The role of wind tunnel modeling in the prediction of wind effects on bridges, *Proceedings of the International Symposium Advances in Bridge Aerodynamics*, Copenhagen, Balkema, Rotterdam.
- Iwan, W.D. and Blevins, R.D. (1974), "A model for the vortex-induced oscillation of structures", *J. Appl. Mech.*, **41**(3), 581-586.

- Larsen, A. (1995), "A generalized model for assessment of vortex-induced vibrations of flexible structures", *J. Wind Eng. Ind. Aerod.*, **57**, 281-294.
- Larsen, A., Eisdahl, S., Andersen, J.E. and Vejrum, T. (2000), "Storebælt suspension bridge vortex shedding excitation and mitigation by guide vanes", *J. Wind Eng. Ind. Aerod.*, **88**(2-3), 283-296.
- Larsen, A., Savage, M., Lafrenière, A., Hui, M.C.H. and Larsen, S.V. (2008), "Investigation of vortex response of a twin box bridge section at high and low Reynolds numbers", *J. Wind Eng. Ind. Aerod.*, **96**(6-7), 934-944.
- Li, M.S., Liao, H.L. and Zheng, S.X. (2009), "A new extreme large boundary layer wind tunnel at Southwest Jiaotong University", *Proceedings of the 7th Asia-Pacific Conference on Wind Engineering*, Taipei, Taiwan.
- Li, M.S. and Tanaka, H. (1996), "Extended joint acceptance function for buffeting analysis", *J. Wind Eng. Ind. Aerod.*, **64**(1), 1-4.
- Li, M.S., Sun Y.G. and Liao, H.L. (2011), "Wind tunnel investigation on vortex-induced vibration for a suspension bridge by section and full aeroelastic modeling", *Proceedings of the 13th International Conference on Wind Engineering (ICWE13)*, Amsterdam, Netherlands.
- Lin, J.C. and Rockwell, D. (1996), "Force identification by vorticity fields: techniques based on flow imaging", *J. Fluid. Struct.*, **10**(6), 663-668.
- Miller, G.D. and Williamson, C.H.K. (1994), "Control of three-dimensional phase dynamics in a cylinder wake", *Exp. Fluids*, **18**(1-2), 26-35.
- Ministry of transport of the people's republic of China (MOT) (2004), *Wind-resistant design specification for highway bridges (JTG/YD60-01-2004)*, China communications press.
- Noca, F., Shiels, D. and Jeon, D. (1999), "A comparison of methods for evaluating time-dependent fluid dynamic forces on bodies, using only velocity fields and their derivatives", *J. Fluid Struct.*, **13**, 551-578.
- Sarwar, M.W. and Ishihara, T. (2010), "Numerical study on suppression of vortex-induced vibrations of box girder bridge section by aerodynamic countermeasures", *J. Wind Eng. Ind. Aerod.*, **98**(12), 701-711.
- Simiu, E. and Scanlan, R.H. (1986), *Wind effects on structures*, 2nd Ed., John Wiley and Sons Inc., New York.
- Wilkinson, R.H. (1981), "Fluctuating pressures on an oscillating square prism. Part II, Spanwise correlation and loading", *Aero. Quarterly*, **32**(2), 111-125.
- Williamson, C.H.K. (1988), "The existence of two stages in the transition to three dimensionality of a cylinder wake", *Phys. Fluids*, **31**, 3165-3168.
- Williamson, C.H.K. and Roshko, A. (1988), "Vortex formation in the wake of an oscillating cylinder", *J. Fluid Struct.*, **2**, 355-381.
- Williamson, C.H.K. (1989), "Oblique and parallel modes of vortex shedding in the wake of a cylinder", *J. Fluid Mech.*, **206**, 579-628.
- Xian, R. (2008), *Spanwise vortex-induced vibration research of long-span bridge girder (in Chinese)*, PhD dissertation, Southwest Jiaotong University, Chengdu, China.
- Zhang, Z.T., Chen, Z.Q. and Cai, Y.Y. (2011), "Vortex-induced oscillations of bridges: linkages between sectional model tests and full bridge responses", *Proceedings of the 13th International Conference on Wind Engineering (ICWE13)*, Amsterdam, Netherlands.
- Zhu, L.D. (2005), "Mass simulation and amplitude conversion of bridge sectional model test for vortex-induced resonance" (in Chinese), *Eng. Mech.*, **22**(5), 204-208.